LIMNOLOGY AND OCEANOGRAPHY
Letters

ASLO
Open Access

Limnology and Oceanography Letters 6, 2021, 243–252

doi: 10.1002/lol2.10199

LETTER

Constraining growth rates and the ratio of living to nonliving particulate carbon using beam attenuation and adenosine-5′-triphosphate at Station ALOHA

Fernanda Henderikx-Freitas [1,2]* *David M. Karl* [1,2] *Karin M. Björkman* [1,2] *Angelicque E. White* [1,2]

[1]Department of Oceanography, University of Hawai'i at Mānoa, Honolulu, Hawai'i; [2]Daniel K. Inouye Center for Microbial Oceanography: Research and Education, University of Hawai'i at Mānoa, Honolulu, Hawai'i

Scientific Significance Statement

The proportion of living microbial biomass relative to total organic carbon is poorly constrained in the global ocean, as is the variability of these parameters over seasonal to multiyear times scales. Yet, such knowledge is key to understanding the pathways and fate of organic matter in the sea. Our use of combined discrete bottle and high resolution optical data allowed us to not only characterize for the first time the variability in the proportion of living and detrital carbon in surface waters of an oligotrophic site over 15+ years, but also to constrain estimates of living particle growth rates that drive the daily cycle of carbon production and loss within the ocean mixed layer. These observations may prove crucial to support mass-balance biogeochemical models aiming to understand particle transformation processes between the well-lit surface and the deep ocean environments.

Abstract

Carbon is not only the foundation of all life on our planet, but also an element that persists in detrital material long after living organisms die. Quantifying the relative amount of living and nonliving carbon in suspended particles in the ocean is challenging and rarely done; yet it is key to understanding the fate of organic matter and informing food web models. Here, we use particulate adenosine-5′-triphosphate (ATP) and particulate carbon (PC) data collected as a component of the Hawaii Ocean Time-series program to show that living particles comprise only ~ 26–42% of the total PC pool in the surface waters of the North Pacific Subtropical Gyre, regardless of time of year. Diel-resolving particulate beam attenuation data are then used in conjunction with PC and ATP data to constrain living particle net growth rates for this system, yielding rates of ~ 0.5–0.7 d^{-1} year-round. These estimates are realistic and consistent with previous microscopy and incubation-based work in the region.

*Correspondence: fhenderi@hawaii.edu

Associate editor: Jeffrey Krause

Author Contribution Statement: A.E.W. and F.H.F. conceived of the work; D.M.K. had the inspiration and perseverance to maintain a 30 year time-series including particulate ATP; F.H.F. wrote the initial draft; F.H.F. and A.E.W. refined the initial manuscript; K.M.B., F.H.F., D.M.K., and A.E.W. collected and analyzed data and/or contributed to data analysis; all authors edited the final manuscript.

Data Availability Statement: Data are available on the Zenodo repository (doi: 10.5281/zenodo.4730697), at https://zenodo.org/record/4730697#.YMKhq_lKiUk.

Additional Supporting Information may be found in the online version of this article.

Total organic carbon in the ocean is distributed among three operationally-defined pools: dissolved organic carbon (which includes colloids and particles < 0.2 μm such as viruses), nonliving particulate organic carbon (e.g., detritus), and living carbon or biomass (Karl and Dobbs 1998). The daily cycles of life and death of ocean microbes largely facilitate the exchange of organic carbon between these three reservoirs (Rochna 1963; Karl et al. 1991; Karl and Dobbs 1998). This makes the sheer mass of living organisms "one of the most important master variables in microbial ecology" (Karl and Dobbs 1998). Yet, the proportion of living microbial biomass in the ocean relative to total organic carbon is poorly constrained, as is how such a parameter varies in situ over seasonal to multi-year times scales. Current estimates of the relative percentage of living carbon within the euphotic zone in the global ocean varies widely, ranging from ~ 30% of the total particulate carbon (PC) in the oligotrophic subtropics to ~ 80–100% in more eutrophic systems (Holm-Hansen and Booth 1966; Gordon 1971; Gordon et al. 1979; Costa-Pierce et al. 1984; Karl and Dobbs 1998; Graff et al. 2015). While the general consensus is that the fraction of living biomass scales onto ocean productivity (although exceptions have been argued, *see* Arteaga et al. 2016), how it varies within an ecosystem is not well known. This is the case largely because there is no direct way to separate living from detrital carbon (Eppley 1968; Laws 2013). Prior efforts to do so have relied on single cell analysis and sorting flow-cytometry, which are time-consuming, laborious, and only able to access a fraction of the microbial population (e.g., < 5 μm; Heldal et al. 2003; Graff et al. 2012, 2015). Indirect proxies for the living component of carbon in the ocean also exist. The concentration of the light-harvesting pigment chlorophyll *a* (Chl *a*) can be used as a proxy for the autotrophic fraction of living cells (e.g., Sathyendranath et al. 2009). However, the carbon to Chl *a* ratio is not constant; cells may alter cellular Chl *a* content as a function of the ambient light and nutrient environment and, hence, Chl *a*-to-phytoplankton carbon ratios may vary by an order of magnitude (e.g., Marra 1997).

The scattering or attenuation of light in situ or as estimated from ocean color satellites have also been used as optical proxies for carbon concentrations (e.g., Behrenfeld et al. 2005). Specifically, the particulate beam attenuation coefficient (c_p), an optical property generally measured at 660 nm, is considered a reliable proxy for in situ PC concentrations (living + nonliving) in oligotrophic waters where particle sizes are roughly constrained between 0.5 and 20 μm (Siegel et al. 1989; Stramski and Kiefer 1991; Gardner et al. 1993; Bishop 1999) and where the shape of the particle size distribution (PSD) does not change significantly over time (Stramski and Kiefer 1991). High frequency observations of c_p have shown that this property oscillates over the diel cycle presenting minimum concentrations around sunrise and maximum concentrations around sunset, reflecting the balance between daytime particle growth due to photosynthesis and nighttime losses such as respiration (Siegel et al. 1989; Cullen et al. 1992; Stramski et al. 1995; Claustre et al. 2008; White et al. 2017). This diel-oscillating portion of the c_p signal is often attributed to the dynamics of living particles, such that its daily amplitude has been shown to correlate with the daily rate of ^{14}C-based carbon fixation in oligotrophic systems (White et al. 2017). This suggests that the amplitude relative to the baseline should also approximate a fraction of the living component of PC but, to our knowledge, this has not been tested.

A more classical approach to measurement of living carbon is via quantification of particulate adenosine-5′-triphosphate (ATP); ATP is a ubiquitous molecule present in all living cells, heterotrophs and autotrophs alike (Holm-Hansen 1973; Karl 1980). Since ATP is present in the cytoplasm, it is not retained by particulate material upon cell death and autolysis, and is not readily adsorbed (Holm-Hansen and Booth 1966); it is considered a reliable proxy for total living microbial biomass, provided that the living carbon : ATP ratio can be approximated within reasonable bounds. This is indeed assumed to be the case; the intracellular concentration of ATP is maintained at a basal level proportional to biovolume (1–2 mM; Karl and Dobbs 1998) suggesting that carbon-to-particulate ATP ratios should be fixed. In a recent reanalysis of ATP as a biomass indicator, Bochdansky et al. (2021) found the mean *C* : ATP ratio measured via five different approaches for the diatom *Thallasiosira weissflogii* (280) to be "remarkably similar to the 250 ratio in Holm-Hansen (1970)" and concluded that "ATP may be the closest metric we have for determining how alive a parcel of water truly is".

ATP is not routinely sampled in the open ocean. However, the Hawaii Ocean Time-series (HOT) program is a notable exception. Since 1989, the HOT program has made near-monthly measurements of particulate ATP throughout the euphotic zone along with other carbon and biomass markers such as total PC concentrations, flow cytometric measurements of picoplankton and heterotrophic bacteria (HBact), and pigment concentrations at Station ALOHA, ~ 100 km north of the island of Oahu, Hawaii (*see* Karl and Church 2017). Since 2015, this program has also obtained high frequency measurements of c_p, providing an unprecedented opportunity to compare independent methods for estimation of biomass and growth of living and detrital material. Here we report the first ever comparison of particulate ATP and optical proxies for carbon composition and detail the time-dependent variability in these fractions in the North Pacific Subtropical Gyre (NPSG) over a 15+ year period.

Methods

Particulate beam attenuation coefficient

Continuous (< 1 min sampling resolution) measurements of the beam attenuation coefficient at 660 nm using a C-Star instrument in flow-through mode (25 cm pathlength, Sea-Bird Scientific) have been collected during HOT cruises at near-

monthly resolution from 2015 to 2020 ($n = 37$ cruises and a total of 92 d; HOT cruises #272–323). HOT cruises last ~ 4 days and are centered at Station ALOHA (22.75°N; 158°W). Sampling periods including transit to and from station were excluded to avoid convolution of spatial variability to the observed signal; thus, each cruise provides ~ 1–3 days of high-resolution, continuous beam attenuation data. The C-Star instrument is operated using a dark optical tube to avoid light contamination, and setup includes a debubbler and a valve control device used to divert water pumped from ~ 7 m depth to a 0.2 μm membrane filter for the first 10 min of every hour to provide background estimates of beam attenuation due to water and dissolved substances (Slade et al. 2010). These blank values were linearly interpolated throughout the cruise and subtracted from the raw measurements to provide particulate beam attenuation coefficients (c_p, m^{-1}). Data were subsequently binned to hourly intervals.

Adequate interpretation of c_p as a proxy for PC requires that the c_p : PC relationship is robust over time. Previous work relying on high-frequency pairs of c_p and PC data in this region (up to 6× per day) showed good correspondence between c_p and PC (slope = 749 ± 98 [mean ± SD] mg C m^{-2}; $r^2 = 0.89$), constant c_p : PC ratio across samples dominated by blooms vs. non-blooms, and no discernable diurnal oscillations in the ratio of c_p : PC (Henderikx-Freitas et al. 2020). Significant changes in the PSD, however, can affect c_p : PC slopes, given that attenuation efficiency is a nonlinear function of particle size (Stramski and Kiefer 1991). The PSD is thought to vary little over the seasonal cycle at Station ALOHA (Barone et al. 2015; White et al. 2015). Particle size data are not readily available to fully test these assumptions on a cruise-to-cruise basis. For these reasons, the analysis relies on the overall patterns of c_p without explicit conversions to PC units, while acknowledging the potential for biases in the c_p : PC relationships affecting specific cruises.

ATP, Chl *a*, PC, and HBact

Sampling of ATP, Chl *a*, PC, and HBact are a routine part of the HOT program core measurement set (https://hahana.soest.hawaii.edu/hot/hot-dogs/). Here, we use all near-monthly (~ 10× per year) ATP ($\mu g\ L^{-1}$), Chl *a* ($\mu g\ L^{-1}$), PC ($\mu g\ L^{-1}$), and HBact (cells L^{-1}) data collected from the top 25 m of the water column via the HOT program from 2003 onwards (HOT cruises #150–307), and processed using standard HOT protocols (*see* Supporting Information S1). This depth horizon is within the mixed layer depth (MLD) 98% of the time (MLD = 62 ± 26 m for the considered period, and is calculated as the first depth where potential density increases by 0.125 kg m^{-3} relative to a 10 m offset). Since cruises last several days, not all variables are collected at the same time within each cruise. For instance, ATP and PC are usually collected at the same time of day, but about a day apart. Comparisons among variables were made on a cruise-to-cruise basis, even if they were not obtained at the exact day or time. In order to reduce variability that may arise from potential diel oscillations, only data from the following time windows were selected for each variable: noon—16:00 h local time (for ATP, PC, and HBact, with 91% of data sampled between 14:00 and 15:00 h), and 19:00-midnight (for Chl *a*, with 92% of data sampled between 20:00 and 21:00 h).

Estimating living C and growth rates from PC, ATP, and c_p data

Here, we assume that the daily increase in c_p or C by proxy reflects a net accumulation factor of living *C* during

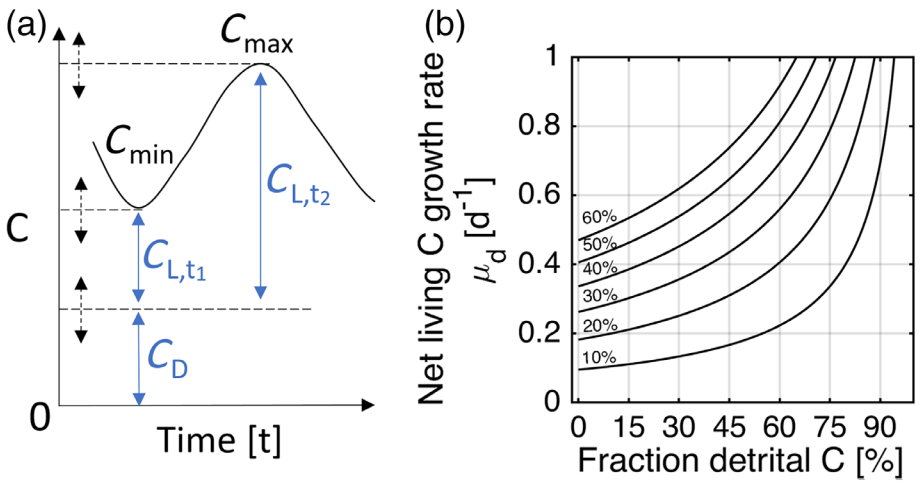

Fig. 1. (**a**) Anatomy of a diel c_p cycle and how measured c_p (or *C*, by proxy) are assumed to be divided into the contribution of living (C_L) and detrital (C_D) carbon components with unknown proportions. C_{min} and C_{max} are the minimum and maximum c_p (or *C*) measured per day, roughly near sunrise and sunset, respectively (*see* Supporting Information S2). (**b**) Net C_L growth rates (μ_d) calculated using Eq. 2 for a selected range of percent daily increases in c_p (e.g., $\alpha = 1.1$–1.6 [or 10–60%]), and different fractions of C_D. Note that daily increases in c_p can represent a wide range of percent C_L provided that μ_d varies accordingly.

daytime (C_{max}/C_{min}), which is proportional to what Claustre et al. (2008) and White et al. (2017) termed "gross community production." The magnitude of c_p reflects the sum of living C (C_L, which includes all autotrophic, mixotrophic, and heterotrophic organisms that can be sensed by the transmissometer based on their size and optical properties, and whose interactions result in net C accumulation during the day), and nonliving C (e.g., detritus, C_D), at unknown proportions in the surface ocean (Fig. 1a). Detritus is defined here as the particulate portion of all non-respiratory C losses from all levels of the food web (Wetzel et al. 1972), assuming autochthonous origin. C_L is assumed to contain both actively growing particles (at various growth rates) as well as viable particles (i.e., capable of DNA synthesis and division) in dormant or senescent modes (Veldhuis et al. 2001; Kirchman 2016). We additionally assume that (1) c_p changes can be linearly related to changes in PC volume over time (White et al. 2017; Henderikx-Freitas et al. 2020); (2) the PSD of living and nonliving pools are similar (no evidence of the contrary is available); (3) the nonliving C pool does not oscillate significantly over the daylight period (e.g., Winn and Karl 1984; Durand and Olson 1996); and (4) the apparent C accumulation during the day is primarily a result of net biological/particle transformation processes (i.e., growth, respiration, grazing, dissolution, aggregation), with sinking, intrusions, and lateral advection assumed to have a negligible role on net changes. Note that an unknown portion of the living C accumulated and lost throughout the daily cycle likely becomes part of the nonliving C pool, and such transformations are implicitly assumed to be contained in the next day's diel cycle amplitude (daily maximum minus daily minimum) and baseline (daily minimum per cruise).

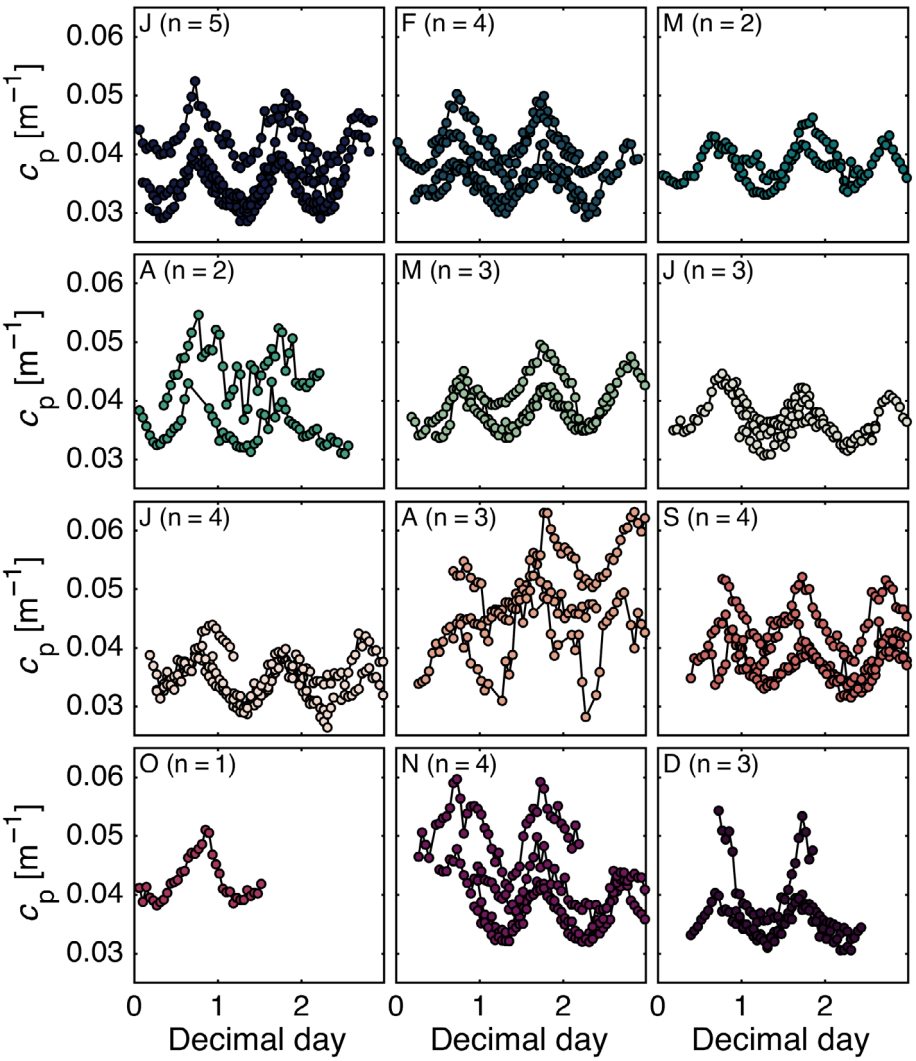

Fig. 2. Time series of hourly averaged particulate beam attenuation (c_p) collected as part of the HOT program at Station ALOHA (2015–2020), aggregated by month (January "J" through December "D", where n = number of cruises per month). Each 1–3 day-long series represents one cruise.

Since the C_L pool may include particles not actively growing during the photoperiod, it is not possible to directly interpret daily percent increases in c_p as increases in percent C_L without knowledge of net particulate C_L growth rates during the daylight period, μ_d (d^{-1}), assuming exponential growth:

$$\mu_d = \frac{1}{t}\ln\left[\frac{C_{max} - C_D}{C_{min} - C_D}\right] \quad (1)$$

where $\left[\frac{C_{max}-C_D}{C_{min}-C_D}\right]$ is equivalent to the fraction of C_L to the total C pool (*see* Fig. 1a). For simplicity, t is considered to be equal to 1 day to reflect growth rates during the day only, thus assuming near steady state over a 24 h period (White et al. 2017; *see* overall symmetric cycles in Fig. 2).

The ratio of ATP (a proxy for living C) to total PC concentrations provides a more direct estimate of the proportion of C_L included in the particulate (> 0.2–202 μm) carbon pool. This requires that ATP concentrations first be converted to C units. Although large variability in C_L : ATP values (~ 100–1000 g g^{-1}) can be found in the literature, values for Station ALOHA have been reported to range between 250 and 400 g C : g ATP (Karl 1980; Christian and Karl 1994); thus, ratios using these two conversion factors are presented as lower and upper bounds of percent C_L estimates (e.g., % C_L = [ATP × m/PC] × 100, where m is either 250 or 400).

The fraction of C_L (or the complementary fraction of detrital C, f) obtained from the ATP analysis can be used in a modification of Eq. 1 to help constrain the net growth rates of C_L implied by the daily accumulation of total C measured via c_p (*see* Fig. 1b). Given that C_{max} can be expressed as αC_{min}, where α is a value larger than 1, and $C_D = fC_{min}$, Eq. 1 can be rewritten as:

$$\mu_d = \frac{1}{t}\ln\left[\frac{\alpha C_{min} - fC_{min}}{C_{min} - fC_{min}}\right] = \frac{1}{t}\ln\left[\frac{\alpha - f}{1 - f}\right] \quad (2)$$

Reliability of the proportions of living and nonliving particles obtained from the ATP and PC data was assessed by checking if realistic values of heterotrophic bacteria carbon quotas, phytoplankton carbon concentrations (PhytoC), and C : Chl a ratios can be implied from the relationships between ATP, PC, HBact, and Chl a, using the inversion approach of Christian and Karl (1994) (*see* Supporting Information S3). Additionally, traditional estimates of growth rates based on ^{14}C assimilation per Chl a and phosphorus uptake rates were obtained to aid interpretation of μ_d (*see* Supporting Information S3).

Results and discussion

High frequency c_p data revealed repeatable diurnal cycles (Figs. 2, 3a) with a 2-fold change in baseline values (Fig. 3b), ~ 3-fold change in amplitudes (Fig. 3c), and no clear seasonality (*see* Supporting Information S4). Consistent with the c_p dataset, ATP data are illustrative of what Venrick (1993) called the "endless summer" of the North Pacific Subtropical Gyre, where seasonality of the surface ocean biomass is muted (Fig. 4a,b). PC and HBact tend to peak in late summer (Fig. 4c-f), and Chl a signals are consistent with phytoplankton photoadaptation processes (Fig. 4g-h), illustrating how Chl a is not a reliable proxy for surface biomass in this region.

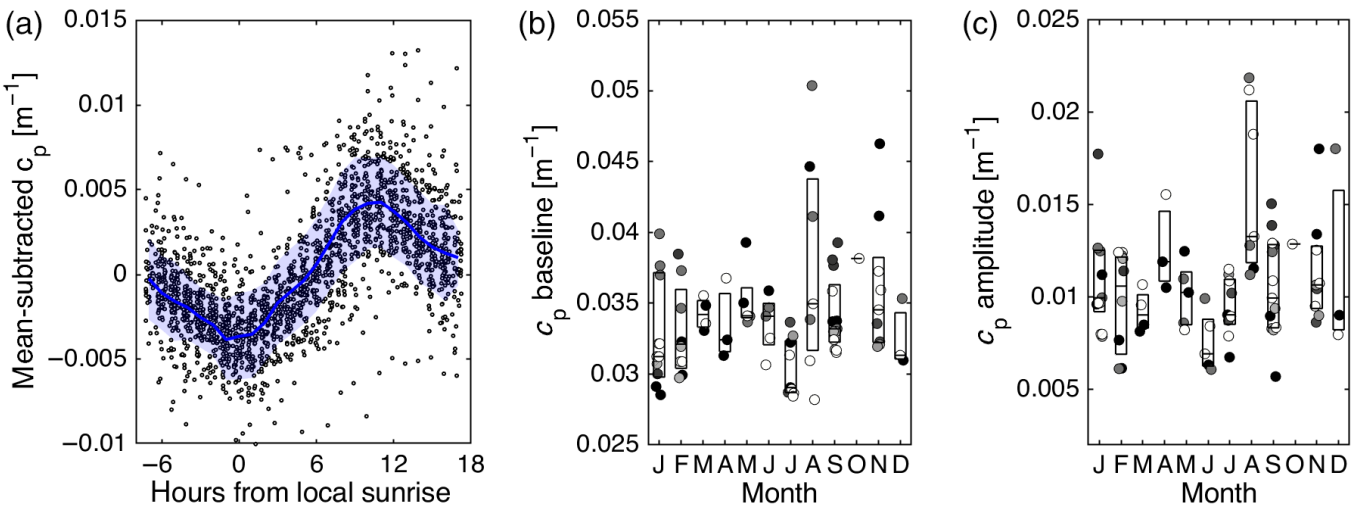

Fig. 3. (**a**) Daily-mean subtracted diel cycles of c_p (dots; same data as in Fig. 2) plotted relative to local sunrise to account for seasonal changes in day length. Blue line and shade represent hourly mean and standard deviation. (**b**) Monthly averages of daily c_p baseline (minimum daily c_p; total n = 76 d); (**c**) monthly averages of daily c_p amplitude (daily max c_p – min c_p). For each month in (b) and (c), circle colors identify values obtained during the same cruise. Box edges mark the 25th and 95th percentiles; horizontal line represents the median for each month.

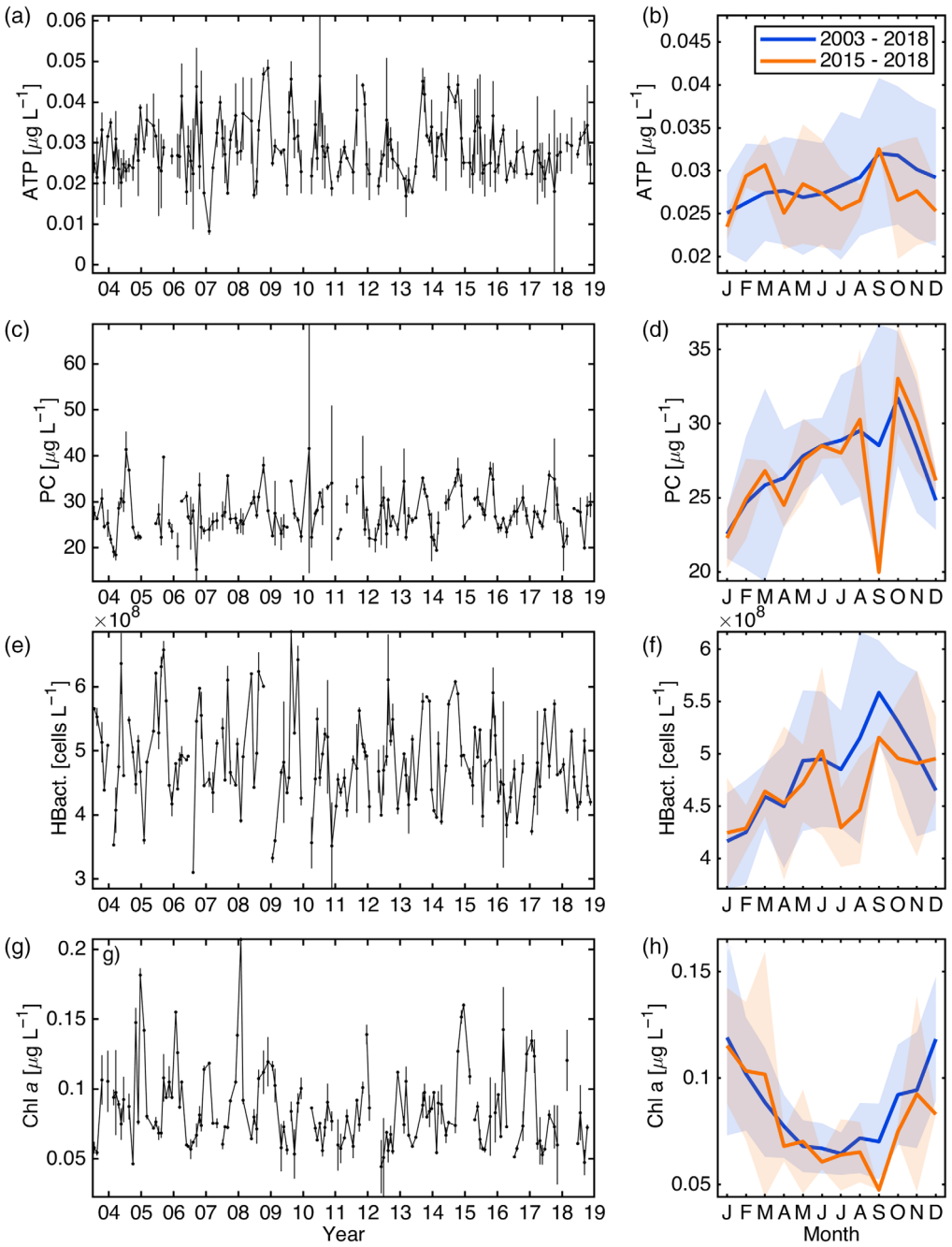

Fig. 4. Time series and climatology of (**a** and **b**) ATP, (**c** and **d**) particulate carbon (PC), (**e** and **f**) heterotrophic bacteria (HBact) cell counts, and (**g** and **h**) Chl *a* averaged over the top 25 m of the water column. Error bars in left panels denote standard deviations over the top 25 m per cruise. Lines and shading on right panels are the monthly top 25 m averages and standard deviations over the entire record (2003–2018, blue), and over the 2015–2018 period (orange).

The daily percent increase in c_p (Fig. 5a) averaged 32 ± 10%, consistent with previous diel-based observations of c_p and PC in the region (White et al. 2017; Henderikx-Freitas et al. 2020). ATP : PC ratios show that between 26 ± 8% (for C_L : ATP = 250) and 42 ± 12% (for C_L : ATP = 400) of particles are living (Fig. 5b). This implies that, on average, the remaining ~ 58–74% are detrital. Percent living *C* estimates showed little month-to-month variability (coefficient of variation = 7%; Fig. 5b).

Validity of the proportions presented in Fig. 5b was assessed via the inversion approach of Christian and Karl (1994). Assuming a C_L : ATP value of 250 yielded average

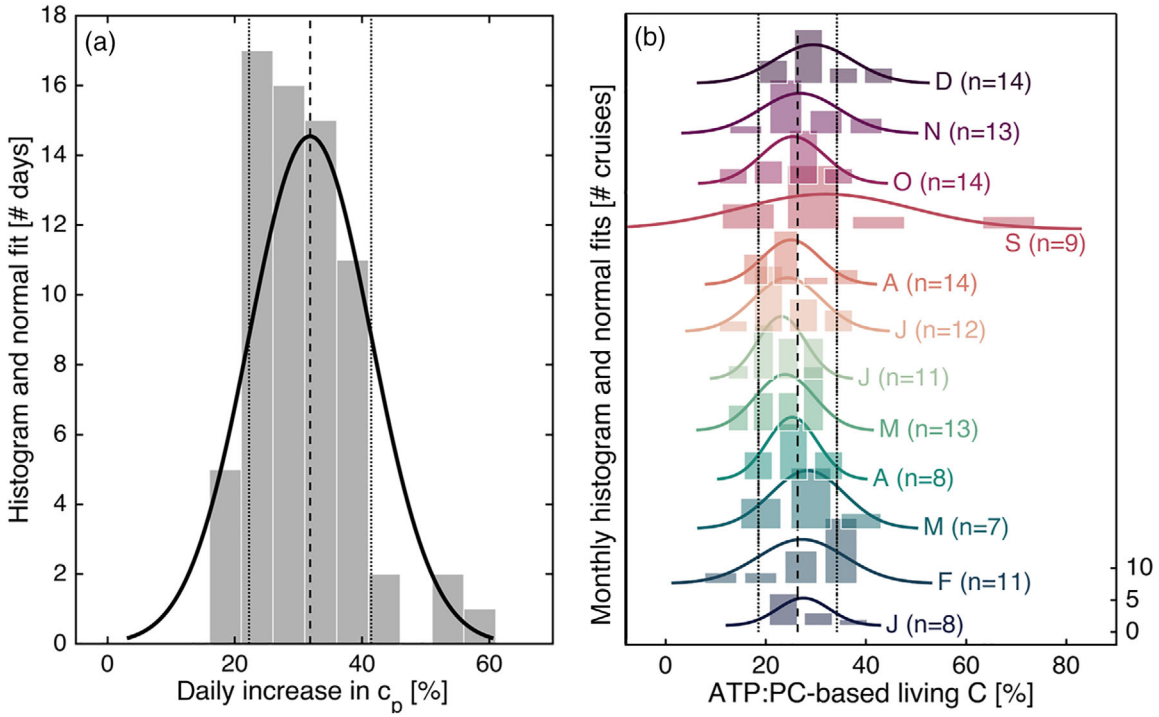

Fig. 5. (**a**) Histogram (bars) and normal distribution fit (line) of daily percent increase in c_p calculated as $[(C_{max} - C_{min})/C_{min}] \times 100$. Vertical dashed lines mark the mean and standard deviation of estimates, 32 ± 10% ($n = 76$). (**b**) Monthly (January, J, through December, D) histograms and normal fits of ATP : PC-based percent living *C*, C_L, for data collected between 2003 and 2018, assuming C_L : ATP of 250 : 1. Vertical dashed lines mark the overall mean and standard deviation for this time period, 26 ± 8% (or 25 ± 5% if only the 2015–2018 period is considered). A C_L : ATP value of 400 would yield average percent C_L estimates of 42 ± 12% for the whole period (2003–2018), and 39 ± 8% for the 2015–2018 period (graphs not shown). Scalebar for staggered histograms is shown to the right of January. *n* indicates the number of cruises per month ($n = 134$ total) where 5–25 m PC and ATP were available within the same cruise since year 2003.

surface *C : Chl a* ratios of 75 ± 21 g g^{-1}, *C* : HBact values of ~ 13 ± 3 fg cell^{-1}, and estimated PhytoC concentrations of ~ 4 ± 2 mg *C* m^{-3} for the May–October period (excluding months of June and September for which coefficients were negative or near zero due to the reduced number of months where ATP, PC, Chl *a*, and HBact data were available simultaneously). Assuming C_L : ATP of 400 yielded average *C* : Chl *a* ratios of 119 ± 34 g g^{-1}, *C* : HBact of ~ 18 ± 4 fg cell^{-1}, and PhytoC of ~ 6 ± 4 mg *C* m^{-3}. Although variability is large, these values are all within the reported *C* : Chl *a* ratios for the surface ocean at Station ALOHA (Christian and Karl 1994), fg cell^{-1} of *C* in HBact from various laboratory studies using local NPSG cultures (Casey et al. 2019; White et al. 2019), and PhytoC estimated from field- and satellite-based studies in the NPSG (Graff et al. 2015; Arteaga et al. 2016), suggesting that the proportion of living particles to the total particulate pool ranging between ~ 26–42% is reasonable. Indeed, percentages are consistent with estimates indicating that living, viable organisms make up ~ 30% of living *C* in oligotrophic regions (e.g., Winn and Karl 1984; Christian and Karl 1994; Graff et al. 2015), and is in agreement with previous descriptions of the PC pool in the open ocean as consisting of "living carbon in a soup of nonliving organic matter" (Karl and Dobbs 1998).

Together, the daily percent increase in total *C* (or c_p) of ~ 30% (Fig. 5a) and detrital *C* fractions averaging 58–74% (Fig. 5b) imply that net growth rates of the living particle pool (μ_d) are constrained between 0.54 and 0.75 d^{-1} (from Eq. 2; Fig. 1b), where a value of 0.69 d^{-1} indicates doubling of biomass over the light cycle. Fully validating the magnitudes of the bulk living particle growth rates and quantifying their variability in situ is impractical, since that would require measuring growth rates for all living populations over relevant time scales. Lab-based estimates of phytoplankton growth rates at Station ALOHA alone have been reported to range anywhere between 0.5 and 2 d^{-1} (Laws et al. 1984; Jones et al. 1996; Laws 2013). Flow cytometry-based studies have also observed a wide range in growth rates of specific nanoplankton (0.6–1.6 d^{-1}; including both autotrophic and heterotrophic organisms > 4–100 μm in diameter; Dugenne et al. 2020), although *Prochlorococcus* and *Synechococcus* (the two most abundant picophytoplankton in the oligotrophic gyres) generally exhibit growth rates of ~ 0.5–0.9 d^{-1} year-round (Liu et al. 1997; Ribalet et al. 2015). Growth rates of heterotrophic

bacteria in the oligotrophic ocean have recently been reported to range between 0.5 and 1.1 d^{-1} (White et al. 2019; Popendorf et al. 2020), but it is not clear to what extent their dynamics are synchronous to that of light-driven organisms. Estimates of net living particle growth rates such as the ones presented here (0.54–0.75 d^{-1}), which represent food-web interactions, should be on the lower end of the phytoplankton-specific growth rates calculated for the region. Furthermore, our estimates reconcile well with incubation-based ^{14}C assimilation per Chl *a* of ~ 80 ± 25 g *C* g^{-1} Chl *a* d^{-1} at Station ALOHA which, along with average *C* : Chl *a* ratios from above suggest average phytoplankton growth rates between 0.47 and 0.74 d^{-1}. Likewise, mean phosphate uptake rates of ~ 4 ± 1 nmol P L^{-1} d^{-1} for surface waters of Station ALOHA, along with particulate phosphate ($P\text{-}PO_4$) pools averaging ~ 12 ± 4 nmol L^{-1} (Björkman et al. 2018), and assuming that the living $P\text{-}PO_4$ pool makes up ~ 50% of the total $P\text{-}PO_4$ pool (D. Karl, personal communication), suggest similar living particle growth rates of 0.52 ± 0.26 d^{-1}.

Living particle growth rates that are comparable to specific growth rates of phytoplankton, along with the likelihood that HBact biomass makes up only a small portion of the particulate ATP and c_p signals due to their low scattering efficiency (in the case of c_p; Stramski and Kiefer 1991) and small size (~ 0.1–0.5 μm) compared to filter size (in the case of ATP), suggests that the % daily increase in c_p reflects, to first order, the dynamics of living plankton. If these conclusions are correct, one would also expect a diel cycle in ATP concentrations to exist in situ. Understanding to which extent different components of the microbial food web are represented by the bulk growth rates, however, is not straightforward since particles may affect the signals in direct and indirect ways. For instance, HBact convert dissolved organic carbon to PC, and also degrade PC (Azam and Hodson 1977), and such transformations are represented in the bulk c_p and ATP signals (White et al. 2017). Similarly, whereas the indirect influence of zooplankton is included in the c_p formulations presented here via daytime grazing dynamics, their direct contribution to total biomass changes may be misrepresented if zooplankton biomass is a large portion of total biomass that consistently peaks at nighttime (White et al. 2017). Contemporaneous tracking of these diverse particle pools would be needed to understand how they affect the net growth rates suggested here. Nonetheless, these results may prove relevant in informing biogeochemical models aiming to characterize particle transformation processes associated with conversions between living and nonliving *C* pools as particles leave the surface mixed-layer.

Competing Interests

The authors declare no competing interests.

References

Arteaga, L., M. Pahlow, and A. Oschlies. 2016. Modeled Chl : C ratio and derived estimates of phytoplankton carbon biomass and its contribution to total particulate organic carbon in the global surface ocean. Global Biogeochem. Cycles **30**: 1791–1810. doi:10.1002/2016GB005458.

Azam, F., and R. E. Hodson. 1977. Dissolved ATP in the sea and its utilisation by marine bacteria. Nature **267**: 696–698. doi:10.1038/267696a0.

Barone, B., R. R. Bidigare, M. J. Church, D. M. Karl, R. M. Letelier, and A. E. White. 2015. Particle distributions and dynamics in the euphotic zone of the North Pacific Subtropical Gyre. J. Geophys. Res. Oceans **120**: 3229–3247. doi:10.1002/2015JC010774.

Behrenfeld, M. J., E. Boss, D. A. Siegel, and D. M. Shea. 2005. Carbon-based ocean productivity and phytoplankton physiology from space. Global Biogeochem. Cycles **19**: GB1006. doi:10.1029/2004GB002299.

Bishop, J. K. B. 1999. Transmissometer measurement of POC. Deep-Sea Res. Part I **46**: 353–369. doi:10.1016/S0967-0637(98)00069-7.

Björkman, K., S. Duhamel, M. Church, and D. M. Karl. 2018. Spatial and temporal dynamics of inorganic phosphate and adenosine-5′-triphosphate in the North Pacific Ocean. Front. Mar. Sci. **5**: 1–14. doi:10.3389/fmars.2018.00235.

Bochdansky, A. B., A. N. Stouffer, and N. N. Washington. 2021. Adenosine triphosphate (ATP) as a metric of microbial biomass in aquatic systems: New simplified protocols, laboratory validation, and a reflection on data from the literature. Limnol. Oceanogr.: Methods **19**: 115–131. doi:10.1002/lom3.10409.

Casey, J. R., K. M. Björkman, S. Ferrón, and D. M. Karl. 2019. Size dependence of metabolism within marine picoplankton populations. Limnol. Oceanogr. **64**: 1819–1827. doi:10.1002/lno.11153.

Christian, J. R., and D. M. Karl. 1994. Microbial community structure at the US-Joint Global Ocean Flux Study Station ALOHA: Inverse methods for estimating biochemical indicator ratios. J. Geophys. Res. **99**: 14269–14276. doi:10.1029/94JC00681.

Claustre, H., Y. Huot, I. Obernosterer, B. Gentili, D. Tailliez, and M. Lewis. 2008. Gross community production and metabolic balance in the South Pacific gyre, using a non-intrusive bio-optical method. Biogeosciences **5**: 463–474. doi:10.5194/bg-5-463-2008.

Costa-Pierce, B. A., D. B. Craven, D. M. Karl, and E. A. Laws. 1984. Correlation of in situ respiration rates and microbial biomass in prawn (*Macrobrachium rosenbergii*) ponds. Aquaculture **37**: 157–168. doi:10.1016/0044-8486(84)90073-5.

Cullen, J. J., M. R. Lewis, C. O. Davis, and R. T. Barber. 1992. Photosynthetic characteristics and estimated growth rates indicate grazing is the proximate control of primary

production in the equatorial Pacific. J. Geophys. Res. Oceans **97**: 639–654. doi:10.1029/91JC01320.

Dugenne, M., F. Henderikx-Freitas, S. T. Wilson, D. M. Karl, and A. E. White. 2020. Life and death of *Crocosphaera* sp. in the Pacific Ocean: Fine scale predator–prey dynamics. Limnol. Oceanogr. **65**: 2603–2617. doi:10.1002/lno.11473.

Durand, M. D., and R. J. Olson. 1996. Contributions of phytoplankton light scattering and cell concentration changes to diel variations in beam attenuation in the equatorial pacific from flow cytometric measurements of pico-, ultra and nanoplankton. Deep-Sea Res. Part II **43**: 891–906. doi:10.1016/0967-0645(96)00020-3.

Eppley, R. W. 1968. An incubation method for estimating the carbon content of phytoplankton in natural samples. Limnol. Oceanogr. **13**: 574–582. doi:10.4319/lo.1968.13.4.0574.

Gardner, W., I. Walsh, and M. Richardson. 1993. Biophysical forcing of particle production and distribution during a spring bloom in the North Atlantic. Deep-Sea Res. Part II **40**: 171–195. doi:10.1016/0967-0645(93)90012-C.

Gordon, D. C. 1971. Distribution of particulate organic carbon and nitrogen at an oceanic station in the central Pacific. Deep-Sea Res. **18**: 1127–1134. doi:10.1016/0011-7471(71)90098-2.

Gordon, D. C., Jr., P. J. Wangersky, and R. W. Sheldon. 1979. Detailed observations on the distribution and composition of particulate organic material at two stations in the Sargasso Sea. Deep-Sea Res. **26**: 1083–1092. doi:10.1016/0198-0149(79)90049-9.

Graff, J. R., A. J. Milligan, and M. J. Behrenfeld. 2012. The measurement of phytoplankton biomass using flow-cytometric sorting and elemental analysis of carbon. Limnol. Oceanogr.: Methods **10**: 910–920. doi:10.4319/lom.2012.10.910.

Graff, J. R., T. K. Westberry, A. J. Milligan, M. B. Brown, G. Dall'Olmo, V. van Dongen-Vogels, K. M. Reifel, and M. J. Behrenfeld. 2015. Analytical phytoplankton carbon measurements spanning diverse ecosystems. Deep-Sea Res. Part I **102**: 6–25. doi:10.1016/j.dsr.2015.04.006.

Heldal, M., D. J. Scanlan, S. Norland, F. Thingstad, and N. H. Mann. 2003. Elemental composition of single cells of various strains of marine *Prochlorococcus* and *Synechococcus* using X-ray microanalysis. Limnol. Oceanogr. **48**: 1732–1743. doi:10.4319/lo.2003.48.5.1732.

Henderikx-Freitas, F., M. Dugenne, F. Ribalet, A. Hynes, B. Barone, D. M. Karl, and A. E. White. 2020. Diel variability of bulk optical properties associated with the growth and division of small phytoplankton in the North Pacific Subtropical Gyre. Appl. Optics **59**: 6702–6716. doi:10.1364/AO.394123.

Holm-Hansen, O. 1970. ATP levels in algal cells as influenced by environmental conditions. Plant Cell Physiol. **11**: 689–700. doi:10.1093/oxfordjournals.pcp.a074557.

Holm-Hansen, O. 1973. The use of ATP determinations in ecological studies. Bull. Ecol. Res. Comm. **17**: 215–233.

Holm-Hansen, O., and C. R. Booth. 1966. The measurement of adenosine triphosphate in the ocean and its ecological significance. Limnol. Oceanogr. **11**: 510–519. doi:10.4319/lo.1966.11.4.0510.

Jones, D. R., D. M. Karl, and E. A. Laws. 1996. Growth rates and production of heterotrophic bacteria and phytoplankton in the North Pacific Subtropical Gyre. Deep-Sea Res. Part I **43**: 1567–1580. doi:10.1016/S0967-0637(96)00079-9.

Karl, D. M. 1980. Cellular nucleotide measurements and applications in microbial ecology. Microbiol. Rev. **44**: 739–796. doi:10.1128/mr.44.4.739-796.1980.

Karl, D. M., and M. J. Church. 2017. Ecosystem structure and dynamics in the North Pacific Subtropical Gyre: New views of an old ocean. Ecosystems **20**: 433–457. doi:10.1007/s10021-017-0117-0.

Karl, D. M., and F. C. Dobbs. 1998. Molecular approaches to microbial biomass estimation in the sea. *In* K. E. Cooksey [ed.], *Molecular approaches to the study of the ocean*. Springer.

Karl, D. M., O. Holm-Hansen, G. T. Taylor, G. Tien, and D. F. Bird. 1991. Microbial biomass and productivity in the western Bransfield Strait, Antarctica during the 1986–87 austral summer. Deep-Sea Res. Part I **38**: 1029–1055. doi:10.1016/0198-0149(91)90095-W.

Kirchman, D. L. 2016. Growth rates of microbes in the oceans. Ann. Rev. Mar. Sci. **8**: 285–309. doi:10.1146/annurev-marine-122414-033938.

Laws, E. A. 2013. Evaluation of in situ phytoplankton growth rates: A synthesis of data from varied approaches. Ann. Rev. Mar. Sci. **5**: 247–268. doi:10.1146/annurev-marine-121211-172258.

Laws, E. A., D. G. Redalje, L. W. Haas, P. K. Bienfang, R. W. Eppley, W. G. Harrison, D. M. Karl, and J. Marra. 1984. High phytoplankton growth and production rates in oligotrophic Hawaiian coastal waters. Limnol. Oceanogr. **29**: 1161–1169. doi:10.4319/lo.1984.29.6.1161.

Liu, H., H. A. Nolla, and L. Campbell. 1997. *Prochlorococcus* growth rate and contribution to primary production in the equatorial and subtropical North Pacific Ocean. Aquat. Microb. Ecol. **12**: 39–47.

Marra, J. 1997. Analysis of diel variability in chlorophyll fluorescence. J. Mar. Res. **55**: 767–784. doi:10.1357/0022240973224274.

Popendorf, K. J., M. Koblížek, and B. A. S. Van Mooy. 2020. Phospholipid turnover rates suggest that bacterial community growth rates in the open ocean are systematically underestimated. Limnol. Oceanogr. **65**: 1876–1890. doi:10.1002/lno.11424.

Ribalet, F., J. Swalwell, S. Clayton, V. Jiménez, S. Sudek, Y. Lin, A. I. Johnson, A. Z. Worden, and E. V. Armbrust. 2015. Light-driven synchrony of *Prochlorococcus* growth and mortality in the subtropical Pacific gyre. Proc. Natl. Acad. Sci. USA **112**: 8008–8012. doi:10.1073/pnas.1424279112.

Rochna, A. G. 1963. Microbiology of detritus of lakes. Limnol. Oceanogr. **8**: 388–393. doi:10.4319/lo.1963.8.4.0388.

Sathyendranath, S., V. Stuart, A. Nair, K. Oka, T. Nakane, H. Bouman, M. H. Forget, H. Maass, and T. Platt. 2009. Carbon-to-chlorophyll ratio and growth rate of phytoplankton in the sea. Mar. Ecol. Prog. Ser. **383**: 73–84. doi:10.1002/lno.10338.

Siegel, D. A., T. Dickey, L. Washburn, M. K. Hamilton, and B. Mitchell. 1989. Optical determination of particulate abundance and production variations in the oligotrophic ocean. Deep-Sea Res. Part I **36**: 211–222. doi:10.1016/0198-0149(89)90134-9.

Slade, W. H., E. Boss, G. Dall'Olmo, M. R. Langner, J. Loftin, M. J. Behrenfeld, and T. K. Westberry. 2010. Underway and moored methods for improving accuracy in measurement of spectral particulate absorption and attenuation. J. Atmos. Oceanic Tech. **27**: 1733–1746.

Stramski, D., and D. A. Kiefer. 1991. Light scattering by microorganisms in the open ocean. Prog. Oceanogr. **28**: 343–383.

Stramski, D., A. Shalapyonok, and R. A. Reynolds. 1995. Optical characterization of the oceanic unicellular cyanobacterium *Synechococcus* grown under a day-night cycle in natural irradiance. J. Geophys. Res. Oceans **100**: 13295–13307.

Veldhuis, M., G. Kraay, and K. Timmermans. 2001. Cell death in phytoplankton: Correlation between changes in membrane permeability, photosynthetic activity, pigmentation and growth. Eur. J. Phycol. **36**: 167–177.

Venrick, E. L. 1993. Phytoplankton seasonality in the central North Pacific: The endless summer reconsidered. Limnol. Oceanogr. **38**: 1135–1149.

Wetzel, R. G., P. H. Rich, M. C. Miller, and H. L. Allen. 1972. Metabolism of dissolved and particulate detrital carbon in a temperate hard-water lake. Mem. 1st Ita. Idrobio. Suppl. **29**: 185–243.

White, A. E., R. M. Letelier, A. L. Whitmire, B. Barone, R. R. Bidigare, M. J. Church, and D. M. Karl. 2015. Phenology of particle size distributions and primary productivity in the North Pacific Subtropical Gyre (Station ALOHA). J. Geophys. Res. Oceans **120**: 7381–7399.

White, A. E., B. Barone, R. Letelier, and D. M. Karl. 2017. Productivity diagnosed from the diel cycle of particulate carbon in the North Pacific Subtropical Gyre. Geophys. Res. Lett. **44**: 3752–3760.

White, A. E., S. J. Giovannoni, Y. Zhao, K. Vergin, and C. A. Carlson. 2019. Elemental content and stoichiometry of SAR11 chemoheterotrophic marine bacteria. Limnol. Oceanogr. **4**: 44–51.

Winn, C. D., and D. M. Karl. 1984. Microbial productivity and community growth rate estimates in the tropical North Pacific Ocean. Biol. Oceanogr. **3**: 123–145.

Acknowledgments

We are grateful for the seagoing support from marine technicians of the HOT program and the many crew of the research vessels, without which this work would not have been possible. Additionally, we are indebted to the Simons Collaboration on Ocean Processes and Ecology (SCOPE) technical staff past and present (Tara Clemente, Tully Rohrer, Tim Burrell, Ryan Tabata, and Eric Shimabukuro) for routine operation of the underway optical sensors in collaboration with the HOT cruises. We also thank John Cullen, Daniel Muratore, Benedetto Barone, and Bob Lansdorp for helpful discussions; Eric Grabowski for quality-checking the PC data; Lance Fujieki for curating the HOT database; and two anonymous reviewers for providing constructive suggestions that helped improve the manuscript. The full HOT database can be accessed at doi:https://hahana.soest.hawaii.edu/hot/hot-dogs/. This work was supported by the National Science Foundation (NSF OCE 1756517 to A.E.W. and D.M.K.) as well as the Simons Foundation (329104 to A.E.W. and D.M.K., 721256 to A.E.W, and 721252 to D.M.K).

Submitted 23 January 2021
Revised 22 May 2021
Accepted 08 June 2021